Available online at www.sciencedirect.com
SCIENCE DIRECT®
Mechanics of Materials 38 (2006) 510–524
MECHANICS OF MATERIALS
www.elsevier.com/locate/mechmat

Macroscopic constitutive law of shape memory alloy thermomechanical behaviour. Application to structure computation by FEM

B. Peultier *, T. Ben Zineb, E. Patoor

Laboratoire de Physique et Mécanique des Matériaux, UMR CNRS 7554, Ecole Nationale Supérieure d'Arts et Métiers, 4 rue Augustin Fresnel, 57078 Metz Cedex 3, France

Received in revised form 23 July 2004

Abstract

In this study, a phenomenological model describing superelasticity, shape memory effect under constant stress and the reorientation process in the martensitic phase is proposed. This model is based on a thermodynamical description of the phase transformation which involves two internal variables: the overall martensite volume fraction and the mean transformation strain. An explicit Gibbs free energy expression is deduced from micromechanical considerations. The evolution laws of the internal variables are derived from this potential, assuming a symmetry of the behaviour between tension and compression and considering only proportional loadings. The behaviour of a representative volume element (RVE) of SMA is deduced and the model is implemented in the ABAQUS finite elements software. Results for uniaxial tensile loadings and a three-point bending test are analysed.

1. Introduction

The unique behaviour of shape memory alloys is barely exploited in traditional engineering. These materials, discovered in the 30s are nowadays the source of unique and innovative applications. These developments involved mostly one-dimensional structures (bar, spring,...) that can be designed empirically, or using the framework of the beam theory (Atanackovic and Achenbach, 1989; Gillet et al., 1995; Tobushi and Tanaka, 1991). In many cases three-dimensional structures are more interesting, but their thermomechanical responses are harder to predict. Numerical simulations using the finite elements method cannot be avoided for the design of these applications. The goal of this work is to develop a model describing the thermomechanical behaviour of SMA that should be implemented into finite element softwares.

A variety of models have been proposed to describe the behaviour of shape memory alloys. Two kinds of approaches can be distinguished: macroscopic phenomenological models and micromechanical ones.

* Corresponding author. Tel.: +33 3 87 37 54 30; fax: +33 3 87 37 54 70.
E-mail address: bertrand.peultier@metz.ensam.fr (B. Peultier).

0167-6636/$ - see front matter © 2005 Elsevier Ltd. All rights reserved.
doi:10.1016/j.mechmat.2005.05.026

Adopting the macroscopic phenomenological point of view, Bekker and Brinson (1998) consider a set of experiments to define the response to different thermo-mechanical loadings. A stress–temperature phase transformation diagram and global kinetic laws describing the transformation behaviour are deduced. Some authors (Leclercq and Lexcellent, 1996; Tanaka et al., 1995) build the phase transformation diagram from a thermodynamical analysis of the martensitic transformation. This allows to define a consistent mathematical description able to predict unidirectional SMA response to arbitrary stress–temperature loading. Those 1D descriptions are usually extended to 3D models by assuming the martensite transformation strain is fully oriented by the current stress state, which is verified only with proportional loadings. Other models (Auricchio and Taylor, 1997; Trochu and Qian, 1997) are built on the similarity between superelasticity and plasticity: the transformation from austenite to martensite appears up to a yield stress and is completed when all the volume is in martensitic phase. Using a framework derived from plasticity techniques, these models are well adapted to finite-element scheme for isothermal loadings. Nevertheless, if temperature influence can be introduced in the yield stress, the shape memory effect is not predicted and also the constrained recovery is used in many applications.

The second approach considers the microstructural aspects of the martensitic transformation (Lagoudas and Bo, 1999; Patoor et al., 1988). Micromechanical study starts at the level of the martensitic variants. At this scale the transformation strain is defined from crystallographical considerations. Twenty four habit plane variants of martensite are distinguished for Cu-based or NiTi SMAs. The volumic fraction of each variant is chosen as internal variable. The free energy function is then determined at the crystal level and is used to derive the behaviour of a single-crystal or an individual grain. Furthermore, the behaviour for polycrystalline SMA is obtained from scale transition methods. Some authors use self-consistent method (Patoor et al., 1996), others integrate over many grains with finite element techniques (Thamburaja and Anand, 2002; Lim and McDowell, 2002). Those models are able to predict superelasticity, shape memory effect and reorientation of martensite within an intrinsic 3D description. But the simulation of complex structures with those models is very restricted due to their computation cost.

The aim of the present work is to simplify a micromechanical model, to obtain an explicit approximation of the free energy of a polycrystalline SMA. Two internal variables are introduced to reach a good approximation of the micromechanical approach: a scalar one, the volumic martensitic fraction in the considered representative volume element and a tensorial one, the mean transformation strain of the martensitic phase volume. From this energy is derived the behaviour of SMA. Constitutive laws and tangent operators are written in a way of implementation into the finite element code ABAQUS. In this paper the model is verified for uniaxial loadings and an application on a three points bending test is analysed.

2. Thermodynamic of SMA

2.1. Internal variables

In this approach the objective is to define an explicit expression of the free energy over a macroscopic volume of SMA. A representative volume element (RVE) of a polycrystalline SMA is considered. Upon a thermomechanical loading, an austenitic domain with volume V_A and a martensitic one with volume V_M are distinguished inside this RVE (Fig. 1).

The martensitic transformation inside the RVE is induced by mechanical or thermal loading, so the macroscopic stress and the temperature, respectively denoted by Σ_{ij} and T, are taken as control variables. The small strain formalism is adopted because the macroscopic reversible strain over a polycrystalline RVE cannot exceed 6%. The thermal dilatation term (~0.01%) is neglected with regard to the transformation one. Assuming the same elastic constants

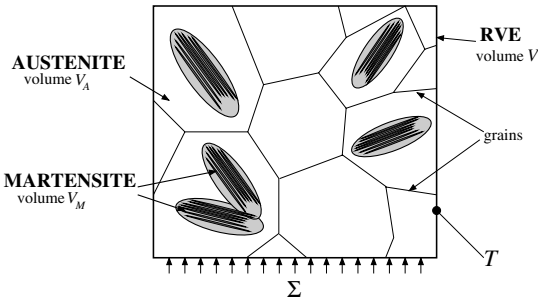

Fig. 1. Representative volume element (RVE). Composed of many austenitic grains where martensitic domains appear according to the thermomechanical loading.

for both phases, one obtains an additive decomposition of the macroscopic total strain into a macroscopic elastic part and a macroscopic transformation part:

$$E_{ij} = E_{ij}^{\mathrm{el}} + E_{ij}^{\mathrm{T}} \tag{1}$$

The macroscopic transformation strain E_{ij}^{T} is equal to the average value of the local transformation strain $\varepsilon_{ij}^{\mathrm{T}}(r)$ over the volume V of the RVE.

$$E_{ij}^{\mathrm{T}} = \frac{1}{V}\int_V \varepsilon_{ij}^{\mathrm{T}}(r)\,\mathrm{d}V \tag{2}$$

Considering that $\varepsilon_{ij}^{\mathrm{T}}(r)$ is defined on the martensitic volume V_{M} and takes null values in the austenitic volume, the macroscopic transformation strain simplifies into:

$$E_{ij}^{\mathrm{T}} = f\bar{\varepsilon}_{ij}^{\mathrm{T}} \tag{3}$$

with $f = \frac{V_{\mathrm{M}}}{V}$ and $\bar{\varepsilon}_{ij}^{\mathrm{T}} = \frac{1}{V_{\mathrm{M}}}\int_{V_{\mathrm{M}}} \varepsilon_{ij}^{\mathrm{T}}(r)\,\mathrm{d}V$.

Here are defined the two internal variables used in this approach: the scalar variable f is the volume fraction of martensite induced during the thermomechanical loading and the tensorial variable $\bar{\varepsilon}_{ij}^{\mathrm{T}}$ is the mean transformation strain defined over the transformed volume V_{M}. This tensor describes the average orientation of the variants of martensite. It is related not only to the phase transformation induced under mechanical and thermal loading, but also to the reorientation of variants due to a mechanical loading in the martensitic state. The internal variable $\bar{\varepsilon}_{ij}^{\mathrm{T}}$ plays a similar role as the remnant polarisation p^{rem} for piezoelectricity (Hwang et al., 1995; Maugin, 1988). These variables account for interface displacement in a multidomain material: p^{rem} for polarized domains in electromechanical coupling and $\bar{\varepsilon}_{ij}^{\mathrm{T}}$ for martensite variants for orientation process in phase transformation.

Due to their physical meaning, internal variables f and $\bar{\varepsilon}_{ij}^{\mathrm{T}}$ are subjected to physical constraints. The martensitic fraction f must be a defined positive quantity that cannot exceed unity. The physical limitations imposed on the tensor of transformation strain are more complex. In this paper, we follow the assumption (Leclercq and Lexcellent, 1996) that the equivalent transformation strain $\bar{\varepsilon}_{\mathrm{eq}}^{\mathrm{T}}$ saturates to a maximal value $\varepsilon_{\mathrm{max}}^{\mathrm{T}}$. In this paper, the Von-Mises equivalent strain and stress are used and the physical constrains of the internal variables are expressed as:

$$0 \leqslant f \leqslant 1 \quad \text{and} \quad \bar{\varepsilon}_{\mathrm{eq}}^{\mathrm{T}} \leqslant \varepsilon_{\mathrm{max}}^{\mathrm{T}} \tag{4}$$

In shape memory alloys the martensitic transformation appends with negligible volume variation and one can consider that the mean transformation strain tensor has not hydrostatic part and must satisfy $\bar{\varepsilon}_{kk}^{\mathrm{T}} = 0$.

2.2. Free energy of the RVE

We consider the Gibb's free energy, noted ψ, function of the stress, the temperature of the internal variables f and $\bar{\varepsilon}_{ij}^{\mathrm{T}}$. This energy results from the contribution of different sources (Patoor et al., 1988):

$$\psi = W_{\mathrm{potential}} - W_{\mathrm{elastic}} - W_{\mathrm{chemical}} - W_{\mathrm{interface}} \tag{5}$$

- $W_{\mathrm{potential}}$ denotes the potential energy related to the total strain.
- W_{elastic} denotes the mechanical energy.
- W_{chemical} denotes the chemical energy related to the phase transformation.
- $W_{\mathrm{interface}}$ is the interfacial energy related to the existence of austenite–martensite interfaces.

The last contribution is usually neglected for thermoelastic shape memory alloy because the plate shape structure of martensite variants suggests that the interfacial energy is negligible with respect to the mechanical energy (Siredey et al., 1999).

$$W_{\mathrm{interface}} = 0 \tag{6}$$

The chemical energy can be described as a linear function of the temperature without any stress dependence. For a unit volume, this energy is defined as:

$$W_{\mathrm{chemical}}(T, f) = B(T - T_0)f \tag{7}$$

where T_0 denotes the thermodynamical equilibrium temperature between austenite and martensite and B is a material constant (Bekker and Brinson, 1998).

For a unit volume the definition of the potential energy is:

$$W_{\mathrm{potential}}\left(\Sigma_{ij}, f, \bar{\varepsilon}_{ij}^{\mathrm{T}}\right) = \Sigma_{ij}E_{ij} = \Sigma_{ij}\mathscr{S}_{ijkl}\Sigma_{kl} + \Sigma_{ij}\bar{\varepsilon}_{ij}^{\mathrm{T}}f \tag{8}$$

with $\mathscr{S}_{ijkl}$ being the four order softness tensor.

Evaluation of the elastic energy is far more complex than for the other contributions. This energy is defined as:

$$W_{\text{elastic}} = \frac{1}{2V}\int_V \sigma_{ij}(r)\varepsilon_{ij}^{\text{el}}(r)\,\mathrm{d}V \tag{9}$$

where $\sigma_{ij}(r)$ and $\varepsilon_{ij}^{\text{el}}(r)$ are the local stress and the elastic strain in each point (r) of the volume V of the RVE.

Using kinematics (Eq. (1)) it is transformed into:

$$W_{\text{elastic}} = \frac{1}{2V}\int_V \sigma_{ij}(r)(\varepsilon_{ij}(r) - \varepsilon_{ij}^{\text{T}}(r))\,\mathrm{d}V \tag{10}$$

and by partial integration and taking into account the boundary conditions it is reduced to (Patoor et al., 1988):

$$W_{\text{elastic}} = \frac{1}{2}\Sigma_{ij}E_{ij} - \frac{1}{2V}\int_V \sigma_{ij}(r)\varepsilon_{ij}^{\text{T}}(r)\,\mathrm{d}V \tag{11}$$

Observation of the microstructure of the RVE shows different characteristic scales in the structure of the material. Three scales can be considered: the overall volume, the grain level and the scale of the variants of martensite inside the grains. Each scale is associated to a stress of different order (I, II, III) (Fig. 2).

$$\sigma_{ij}(r) = \sigma_{ij}^{\text{I}} + \sigma_{ij}^{\text{II}}(r) + \sigma_{ij}^{\text{III}}(r) \tag{12}$$

- The stress of order I, $\sigma_{ij}^{\text{I}} = \frac{1}{V}\int_V \sigma_{ij}(r)\,\mathrm{d}V = \Sigma_{ij}$, is the average stress over the volume V and corresponds to the macroscopic stress applied to the RVE.
- The stress of order II, $\sigma_{ij}^{\text{II}}(r) = \frac{1}{V_N}\int_{V_N} \sigma_{ij}(r)\,\mathrm{d}V - \sigma_{ij}^{\text{I}}$, is the fluctuation between the average stress of the grain N and the global stress σ_{ij}^{I} due to the incompatibilities between deformed grains.
- The stress of order III, $\sigma_{ij}^{\text{III}}(r) = \sigma_{ij}(r) - \sigma_{ij}^{\text{II}}(r) - \sigma_{ij}^{\text{I}}$, is the fluctuation of the stress at the point (r) inside the grain N, due to the incompatibilities between the variants of martensite into the austenitic matrix.

Introducing the decomposition of the stress (12) into the expression of the elastic energy (9) three contributions can be distinguished:

$$W_{\text{elastic}} = W_{\text{macroscopic}} + W_{\text{intergranular}} + W_{\text{intervariant}} \tag{13}$$

- The macroscopic elastic energy:

$$W_{\text{macroscopic}} = \frac{1}{2}\Sigma_{ij}E_{ij} - \frac{1}{2V}\int_V \sigma_{ij}^{\text{I}}(r)\varepsilon_{ij}^{\text{T}}(r)\,\mathrm{d}V = \frac{1}{2}\Sigma_{ij}E_{ij}^{\text{el}}$$

- The intergranular interaction energy:

$$W_{\text{intergranular}} = -\frac{1}{2V}\int_V \sigma_{ij}^{\text{II}}(r)\varepsilon_{ij}^{\text{T}}(r)\,\mathrm{d}V$$

- The intervariant interaction energy:

$$W_{\text{intervariant}} = -\frac{1}{2V}\int_V \sigma_{ij}^{\text{III}}(r)\varepsilon_{ij}^{\text{T}}(r)\,\mathrm{d}V$$

In the next two paragraphs, different assumptions will be used to reach a macroscopic approximation of the last two terms estimated from micromechanical and homogenisation results.

2.2.1. Estimation of the intergranular energy

In this section, we focus on the granular structure, $\sigma_{ij}^{\text{II}}(r)$ is a step-wise function having a constant value $\sigma_{ij}^{\text{II}}(N)$ over a grain N. So the integral expression of the intergranular energy of the RVE simplifies into the sum of the contribution of each grain:

$$W_{\text{intergranular}} = -\frac{1}{2V}\int_V \sigma_{ij}^{\text{II}}(r)\varepsilon_{ij}^{\text{T}}(r)\,\mathrm{d}V = -\frac{1}{2}\sum_N \sigma_{ij}^{\text{II}}(N)\varepsilon_{ij}^{\text{T}}(N)\frac{V_N}{V} \tag{14}$$

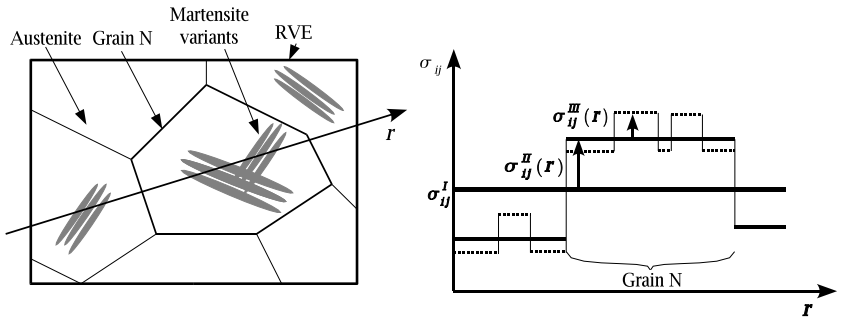

Fig. 2. Decomposition of the stress into first, second or third order from microstructural considerations.

with $\varepsilon_{ij}^{\mathrm{T}}(N) = \frac{1}{V_N}\int_{V_N}\varepsilon_{ij}^{\mathrm{T}}(r)\,\mathrm{d}V$ being the average transformation strain over the grain N.

Let us consider a grain undergoing a transformation strain $\varepsilon_{ij}^{\mathrm{T}}(N)$. By assuming this grain is an ellipsoidal inclusion inside a medium having a macroscopic transformation strain E_{ij}^{T}, one can express the stress $\sigma_{ij}^{\mathrm{II}}(N)$ from the Kröner solution of this problem (Kröner, 1961):

$$\sigma_{ij}^{\mathrm{II}}(N) = C_{ijmn}\left(I_{mnkl} - \mathbf{S}_{mnkl}^{\mathrm{esh}}(N)\right)\left(E_{kl}^{\mathrm{T}} - \varepsilon_{kl}^{\mathrm{T}}(N)\right) \quad (15)$$

with C_{ijmn} being the elastic tensor, I_{mnkl} the identity tensor and $\mathbf{S}_{mnkl}^{\mathrm{esh}}(N)$ the Eshelby tensor of the grain N.

Including (15) into (14), the intergranular energy becomes:

$$\begin{aligned} W_{\mathrm{intergranular}} &= -\frac{1}{2}\sum_N C_{ijmn}\left(I_{mnkl} - \mathbf{S}_{mnkl}^{\mathrm{esh}}(N)\right)E_{kl}^{\mathrm{T}}\varepsilon_{ij}^{\mathrm{T}}(N)\frac{V_N}{V} \\ &\quad + \frac{1}{2}\sum_N C_{ijmn}\left(I_{mnkl} - \mathbf{S}_{mnkl}^{\mathrm{esh}}(N)\right)\varepsilon_{kl}\varepsilon_{ij}^{\mathrm{T}}(N)\frac{V_N}{V} \end{aligned} \quad (16)$$

The first term corresponds to the interaction of the volume of the RVE on the local grain N. By considering that every grain has a similar shape or at least a similar aspect ratio, it is assumed that the Eshelby tensor $\mathbf{S}_{mnkl}^{\mathrm{esh}}(N)$ is identical for each grain.

$$\begin{aligned} &-\frac{1}{2}\sum_N C_{ijmn}\left(I_{mnkl} - \mathbf{S}_{mnkl}^{\mathrm{esh}}(N)\right)E_{kl}^{\mathrm{T}}\varepsilon_{ij}^{\mathrm{T}}(N)\frac{V_N}{V} \\ &= -\frac{1}{2}C_{ijmn}\left(I_{mnkl} - \mathbf{S}_{mnkl}^{\mathrm{esh}}(N)\right)E_{kl}^{\mathrm{T}}E_{ij}^{\mathrm{T}} \end{aligned} \quad (17)$$

The second term in relation (16) is the auto-interaction of the grain N on itself. In first approximation this term is supposed identical for each grain with a transformation strain $\varepsilon_{ij}^{\mathrm{T}}(N)$ which takes the average value over the RVE E_{ij}^{T}. Moreover the grains are assumed to have the same volume V_N:

$$\begin{aligned} &-\frac{1}{2}\sum_N C_{ijmn}\left(I_{mnkl} - \mathbf{S}_{mnkl}^{\mathrm{esh}}(N)\right)\varepsilon_{kl}^{\mathrm{T}}(N)\varepsilon_{ij}^{\mathrm{T}}(N)\frac{V_N}{V} \\ &\approx -\frac{1}{2}\frac{V}{V_N}C_{ijmn}\left(I_{mnkl} - \mathbf{S}_{mnkl}^{\mathrm{esh}}(N)\right)E_{kl}^{\mathrm{T}}E_{ij}^{\mathrm{T}} \end{aligned} \quad (18)$$

The two terms (17) and (18) of the intergranular energy (16) are regrouped introducing a "hardening" tensor H_{ijkl}. In first approximation this tensor is supposed to take the form $H_{\mathrm{grain}}\cdot I_{ijkl}$. Eq. (16) simplifies into:

$$W_{\mathrm{intergranular}} = \frac{1}{2}H_{\mathrm{grain}}E_{ij}^{\mathrm{T}}E_{ij}^{\mathrm{T}} = \frac{1}{2}H_{\mathrm{grain}}\bar{\varepsilon}_{ij}^{\mathrm{T}}\bar{\varepsilon}_{ij}^{\mathrm{T}}f^2 \quad (19)$$

These different assumptions lead to neglect the influence of the crystallography on the transformation but they allow to estimate the intergranular energy introducing only one material parameter H_{grain}.

2.2.2. Estimation of the intervariant energy

In this section, we focus on the martensitic microstructure inside grains. We consider the intervariant energy as the energy related to the internal stress of order III $\sigma_{ij}^{\mathrm{III}}(r)$. The intervariant energy $w_{\mathrm{intervariant}}^N$ into a grain N is defined as:

$$w_{\mathrm{intervariant}}^N = -\frac{1}{2V_N}\int_{V_N}\sigma_{ij}^{\mathrm{III}}(r)\varepsilon_{ij}^{\mathrm{T}}(r)\,\mathrm{d}V \quad (20)$$

The global intervariant energy of the RVE is the sum over all the grains of the energy of interaction between variants inside each grain N:

$$W_{\mathrm{intervariant}} = \sum_N w_{\mathrm{intervariant}}^N\frac{V_N}{V} \quad (21)$$

By a micromechanical analysis of the thermoelastic behaviour of a SMA grain, Siredey gives an expression of the intervariant interaction energy over one parent phase crystal (Niclaeys et al., 2002; Siredey et al., 1999):

$$w_{\mathrm{intervariant}}^N = \frac{1}{2}\sum_{m,n} f_m\mathscr{H}^{mn}f_n \quad (22)$$

where f_n is the volumic fraction of the variant n and $\mathscr{H}^{mn}$ the interaction energy coefficient between variants n and m. This coefficient takes two values depending on the compatibility or incompatibility of the variants n and m considered. This expression is a quadratic function of the volumic fractions f_n of the martensite variants.

From this result and in order to propose a macroscopic estimation for this energy, two assumptions are assumed. Firstly it is supposed that during all the loading the same variants are selected and their volumic fractions evaluated proportionally. Secondly the intervariant energy $w_{\mathrm{intervariant}}^N$ is assumed to be identical in each grain. The expression (22) simplifies into a quadratic function of f:

$$W_{\mathrm{intervariant}} = \frac{1}{2}H_{\mathrm{variant}}f^2 \quad (23)$$

These hypotheses are reasonable only for proportional loadings and neglect the influence of the crystallography. But expression (23) introduces only one

macroscopic material parameter H_{variant}, that is consistent with the objective of building a macroscopic model.

2.2.3. Free energy function

The expression of the elastic energy over the RVE results from the combination of contributions (23) and (19) with relation (13):

$$W_{\text{elastic}} = \frac{1}{2}\Sigma_{ij}E^{\text{el}}_{ij} + \frac{1}{2}H_{\text{grain}}\bar{\varepsilon}^{\text{T}}_{ij}\bar{\varepsilon}^{\text{T}}_{ij}f^2 + \frac{1}{2}H_{\text{variant}}f^2 \tag{24}$$

Introducing (6)–(8) and (24) in the relation (5) gives an explicit macroscopic expression for the free energy:

$$\begin{aligned}\psi\left(\Sigma_{ij},T,f,\bar{\varepsilon}^{\text{T}}_{ij}\right) &= \frac{1}{2}\Sigma_{ij}\mathscr{S}_{ijkl}\Sigma_{kl} + \Sigma_{ij}\bar{\varepsilon}^{\text{T}}_{ij}f - B(T-T_0)f \\ &\quad - \frac{1}{2}H_{\text{grain}}\bar{\varepsilon}^{\text{T}}_{ij}\bar{\varepsilon}^{\text{T}}_{ij}f^2 - \frac{1}{2}H_{\text{variant}}f^2\end{aligned} \tag{25}$$

In SMAs the martensitic transformation occurs with a negligible volume variation. So the mean transformation strain tensor has no hydrostatic part $\bar{\varepsilon}^{\text{T}}_{kk} = 0$ and the term $\Sigma_{ij}\bar{\varepsilon}^{\text{T}}_{ij}$ simplifies in $S_{ij}\bar{\varepsilon}^{\text{T}}_{ij}$, where $S_{ij} = \Sigma_{ij} - \delta_{ij}\frac{\Sigma_{kk}}{3}$ denotes the deviatoric part of the stress.

$$\begin{aligned}\psi\left(\Sigma_{ij},T,f,\bar{\varepsilon}^{\text{T}}_{ij}\right) &= \frac{1}{2}\Sigma_{ij}\mathscr{S}_{ijkl}\Sigma_{kl} + S_{ij}\bar{\varepsilon}^{\text{T}}_{ij}f - B(T-T_0)f \\ &\quad - \frac{1}{2}H_{\text{grain}}\bar{\varepsilon}^{\text{T}}_{ij}\bar{\varepsilon}^{\text{T}}_{ij}f^2 - \frac{1}{2}H_{\text{variant}}f^2\end{aligned} \tag{26}$$

From this expression of the free energy one can now derive a macroscopic analytical constitutive law of the SMA.

3. Constitutive law of SMA

To define the behaviour of the RVE, one has to determine the evolution of the internal variables $\mathrm{d}f$ and $\mathrm{d}\bar{\varepsilon}^{\text{T}}_{ij}$ due to a modification of the control variables $\mathrm{d}\Sigma_{ij}$ and $\mathrm{d}T$. This is done by optimising the Gibbs free energy ψ as a function of the two internal variables. The optimisation must take into account the physical limitations of the internal variables, see Eq. (4). Those kinematic constraints are introduced using the Kuhn and Tucker optimisation conditions. Let us define the Lagrangian function $L(\Sigma_{ij},T,f,\bar{\varepsilon}^{\text{T}}_{ij})$ based on the Gibbs energy $\psi(\Sigma_{ij},T,f,\bar{\varepsilon}^{\text{T}}_{ij})$. Three Lagrange multipliers λ_0, λ_1 and λ_2 are introduced, two associated to the martensitic volume fraction and one associated to the mean transformation strain. These quantities are defined positive or null and must satisfy the following conditions:

$$\lambda_0(0-f) = 0, \quad \lambda_1(f-1) = 0 \quad \text{and} \quad \lambda_2\left(\bar{\varepsilon}^{\text{T}}_{\text{eq}} - \varepsilon^{\text{T}}_{\max}\right) = 0 \tag{27}$$

The Lagrangian function is written as:

$$\begin{aligned}L\left(\Sigma_{ij},T,f,\bar{\varepsilon}^{\text{T}}_{ij}\right) &= \psi\left(\Sigma_{ij},T,f,\bar{\varepsilon}^{\text{T}}_{ij}\right) + \lambda_0 f - \lambda_1(f-1) \\ &\quad - \lambda_2\left(\bar{\varepsilon}^{\text{T}}_{\text{eq}} - \varepsilon^{\text{T}}_{\max}\right)\end{aligned} \tag{28}$$

The optimum of the Lagrangian function is reached at the point $(f,\bar{\varepsilon}^{\text{T}}_{ij})$ where its gradient is null. This gradient has two components associated to the two internal variables. These components are the thermodynamical forces:

- the transformation force:

$$\begin{aligned}F_f &= \frac{\partial L}{\partial f}\left(\Sigma_{ij},T,f,\bar{\varepsilon}^{\text{T}}_{ij}\right) \\ F_f\left(\Sigma_{ij},T,f,\bar{\varepsilon}^{\text{T}}_{ij}\right) &= S_{ij}\bar{\varepsilon}^{\text{T}}_{ij} - B(T-T_0) \\ &\quad - H_{\text{grain}}\bar{\varepsilon}^{\text{T}}_{ij}\bar{\varepsilon}^{\text{T}}_{ij}f - H_{\text{variant}}f \\ &\quad + \lambda_0 - \lambda_1\end{aligned} \tag{29}$$

- the orientation force:

$$\begin{aligned}F_{\varepsilon_{ij}} &= \frac{\partial L}{\partial \bar{\varepsilon}^{\text{T}}_{ij}}\left(\Sigma_{ij},T,f,\bar{\varepsilon}^{\text{T}}_{ij}\right) \\ F_{\varepsilon_{ij}}\left(\Sigma_{ij},T,f,\bar{\varepsilon}^{\text{T}}_{ij}\right) &= S_{ij}f - H_{\text{grain}}\bar{\varepsilon}^{\text{T}}_{ij}f - \lambda_3\frac{\partial \bar{\varepsilon}^{\text{T}}_{\text{eq}}}{\partial \bar{\varepsilon}^{\text{T}}_{ij}}\end{aligned} \tag{30}$$

Based on the two thermodynamical forces (29) and (30) and the kinematic relations (27), one can define a transformation criterion and an orientation criterion and build the state diagram. Then the evolution laws of the internal variables are deduced from the consistency conditions of the activated mechanisms (transformation and/or orientation). Finally the particular case of partial loadings is analysed.

3.1. Transformation criterion

To take into account the hysteresis of the martensitic transformation into the thermodynamical

equilibrium of the transformation force, one has to introduce a critical transformation force F_f^{critical}. Consequently direct transformation will be activated when the transformation force has reached its critical value with respect to the kinematic constraints on the martensitic fraction are not reached:

- transformation $A \rightarrow M$ when: $F_f = F_f^{\text{critical}}$ and $\mathrm{d}F_f > 0$ and $f > 0$ and $f < 1$.

At the opposite, the forward transformation will be activated when the transformation force has reached the opposite critical value:

- transformation $M \rightarrow A$ when: $F_f = -F_f^{\text{critical}}$ and $\mathrm{d}F_f < 0$ and $f > 0$ and $f < 1$.

Otherwise no martensitic transformation occurs:

- no transformation when: $-F_f^{\text{critical}} < F_f < F_f^{\text{critical}}$ or $f = 0$ or $f = 1$.

3.2. Orientation criterion

One has to define the thermodynamical equilibrium of the orientation force which is a tensorial quantity. In this work, two assumptions are done. Firstly the loadings are supposed proportional so the transformation strain is considered as fully oriented by the stress (Leclercq and Lexcellent, 1996):

$$\bar{\varepsilon}_{ij}^{\mathrm{T}} = \frac{3}{2}\eta_{ij}^{\sigma}\bar{\varepsilon}_{\mathrm{eq}}^{\mathrm{T}} \tag{31}$$

with the stress direction $\eta_{ij}^{\sigma} = \frac{S_{ij}}{\Sigma_{\mathrm{eq}}}$, the stress deviator $S_{ij} = \Sigma_{ij} - \delta_{ij}\frac{\Sigma_{kk}}{3}$ and Σ_{eq} the equivalent stress.

Secondly, the Von Mises equivalents for strain and stress are used, despite the dissymmetry observed between tension and compression tests: $\bar{\varepsilon}_{\mathrm{eq}}^{\mathrm{T}} = \sqrt{\frac{2}{3}\bar{\varepsilon}_{ij}^{\mathrm{T}}\bar{\varepsilon}_{ij}^{\mathrm{T}}}$ and $\Sigma_{\mathrm{eq}} = \sqrt{\frac{3}{2}S_{ij}S_{ij}}$.

Consequently the orientation force (30) turns into a scalar expression:

$$F_{\varepsilon_{\mathrm{eq}}}\left(\Sigma_{ij}, T, f, \bar{\varepsilon}_{ij}^{\mathrm{T}}\right) = \Sigma_{\mathrm{eq}} f - H_{\mathrm{grain}}\bar{\varepsilon}_{\mathrm{eq}}^{\mathrm{T}} f^2 - \lambda_3 \tag{32}$$

In this paper, no critical orientation force is introduced. So the orientation process will be activated as soon as the orientation force has reached a null value while respecting the kinematical constraints on the mean transformation strain:

- Orientation of the martensite phase when: $F_{\varepsilon_{\mathrm{eq}}} = 0$ and $\mathrm{d}F_{\varepsilon_{\mathrm{eq}}} > 0$ and $\bar{\varepsilon}_{\mathrm{eq}}^{\mathrm{T}} < \varepsilon_{\mathrm{max}}^{\mathrm{T}}$.
- Otherwise no modification of the orientation of the martensite when: $F_{\varepsilon_{\mathrm{eq}}} < 0$ or $\bar{\varepsilon}_{\mathrm{eq}}^{\mathrm{T}} = \varepsilon_{\mathrm{max}}^{\mathrm{T}}$.

3.3. Transformation state diagram

Based on the transformation and the orientation criterions, the state diagram of the martensitic transformation can be drawn in the space of the control variables (Σ_{ij}, T). This diagram shows the limits of transformation and also the limits of orientation of the martensite (Fig. 3). Three characteristic lines are observed:

- the line defining the beginning of the direct transformation for $f = 0$ and $F_f = F_f^{\text{critical}}$.
- the line of end of the transformation for $f = 1$ and $F_f = F_f^{\text{critical}}$.
- the line defining the limit of saturation of the orientation for $\bar{\varepsilon}_{\mathrm{eq}}^{\mathrm{T}} = \varepsilon_{\mathrm{max}}^{\mathrm{T}}$ and $F_{\varepsilon_{\mathrm{eq}}} = 0$.

The first two lines are related to the phase transformation itself and the third line is associated to the saturation of the mean transformation strain. At high stress level, the martensite phase is fully oriented by the stress and at lower stress level it is only partially oriented by the stress.

This diagram shows non-linear transformation limits at low stress level that can be compared to the one calculated by Zhang and McCormick (2000) and with the experimental one measured by Bekker and Brinson (1998) and Wu et al. (2003).

The combination of the thermodynamical criterions generate a variety of behaviours that can be grouped into only three classes of behaviour:

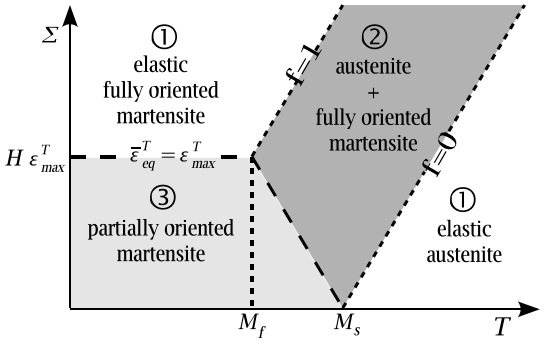

Fig. 3. Transformation diagram of the direct transformation $A \rightarrow M$. Transformation limits in dotted lines. Orientation limits in dashed lines.

1. Elasticity of austenite and martensite: ($-F_f^{\text{critical}} < F_f < F_f^{\text{critical}}$ or $f = 0$ or $f = 1$) and ($F_{\varepsilon_{\text{eq}}} < 0$ or $\bar{\varepsilon}_{\text{eq}}^{\text{T}} = \varepsilon_{\text{max}}^{\text{T}}$).
2. Transformation at constant orientation/saturated orientation: $F_f = \pm F_f^{\text{critical}}$ and $f > 0$ and $f < 1$ and ($F_{\varepsilon_{\text{eq}}} < 0$ or $\bar{\varepsilon}_{\text{eq}}^{\text{T}} = \varepsilon_{\text{max}}^{\text{T}}$).
3. Transformation and orientation of the martensitic: $F_f = \pm F_f^{\text{critical}}$ and $f > 0$ and $f < 1$ and $F_{\varepsilon_{\text{eq}}} = 0$ and $\bar{\varepsilon}_{\text{eq}}^{\text{T}} < \varepsilon_{\text{max}}^{\text{T}}$. As shown in Section 3.4 this class of behaviour also describe the pure process of reorientation of the martensitic phase without transformation: $F_{\varepsilon_{\text{eq}}} = 0$ and ($-F_f^{\text{critical}} < F_f < F_f^{\text{critical}}$ or $f = 1$). In the case $f = 0$, there is not any martensite in the RVE and the austenite behaves elastically (behaviour (1)).

This analysis allows to determine what kind of mechanisms are activated (transformation and/or orientation) for a given thermomechanical loading. Then the evolution laws of the internal variables are deduced from the resolution of the consistency conditions.

3.4. Evolution laws

For each of the three classes of behaviour the evolution laws of the internal variables are different:

1. Class of elastic behaviour: $\mathrm{d}f = 0$ and $\mathrm{d}\bar{\varepsilon}_{\text{eq}}^{\text{T}} = 0$.
2. Transformation at constant orientation: $\mathrm{d}\bar{\varepsilon}_{\text{eq}}^{\text{T}} = 0$, the resolution of the consistency condition of the transformation force $\mathrm{d}F_f = \pm \mathrm{d}F_f^{\text{critical}}$ gives $\mathrm{d}f$.
3. Transformation and orientation: the resolution of the system of equation

$$\begin{cases} \mathrm{d}F_{\varepsilon_{\text{eq}}} = 0 \\ \mathrm{d}F_f = \pm \mathrm{d}F_f^{\text{critical}} \end{cases}$$

gives

$$\begin{cases} \mathrm{d}\bar{\varepsilon}_{\text{eq}}^{\text{T}} \\ \mathrm{d}f \end{cases} \quad \text{while } \mathrm{d}\bar{\varepsilon}_{ij}^{\text{T}} = \frac{3}{2}\mathrm{d}\bar{\varepsilon}_{\text{eq}}^{\text{T}}\eta_{ij}^{\sigma}$$

This solution can be extended to the case of orientation without transformation: by solving the system one can find that $\mathrm{d}f$ is independent from $\mathrm{d}\bar{\varepsilon}_{\text{eq}}^{\text{T}}$, and imposing $\mathrm{d}f = 0$ does not modify the expression of $\mathrm{d}\bar{\varepsilon}_{\text{eq}}^{\text{T}}$.

In the case of complete transformation loadings, the critical transformation force F_f^{critical} is kept constant and $\mathrm{d}F_f^{\text{critical}} = 0$. In the more general case of partial loadings, one must take into account the evolution of F_f^{critical} with the loading.

3.5. Partial loadings

In most applications, only a partial loading is imposed so it is important to be able to describe not only the major loop but also the sub-loops. The notion of partial loading is usually regarded only from the point of view of the volume fraction of martensite. Sub-loops appear when an unloading occurs while the material is partially transformed such as when the volume fraction is smaller than one.

Fig. 4 shows that in sub-loops the forward transformation appends earlier than the major forward loop. Moreover it depends on the quantity of martensite formed during the previous direct transformation. This effect is taken into account introducing a variable critical transformation force, function of the fraction of martensite at the beginning of the forward loop f^* (Fig. 5a). Gillet gives the following expression of the critical transformation force (Gillet et al., 1995):

$$F_f^{\text{critical}} = F_f^{\max}(1 - 2f^*) \tag{33}$$

This relation defines the locus of the beginning of the forward transformation for superelastic loadings but is not able to describe sub-loops observed in thermal loadings. In the present approach using two internal variables, the critical force must not only be a function of the fraction of martensite but also of the orientation of the martensite. In this framework, the forward transformation is considered as a sub-loop when the fraction of martensite is lower than one or when the mean transformation strain has not reached its maximal value $\varepsilon_{\text{max}}^{\text{T}}$. The

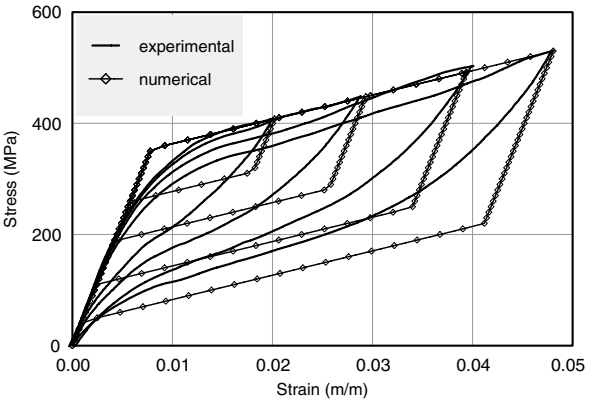

Fig. 4. Sub-loops in a superelastic NiTi wire.

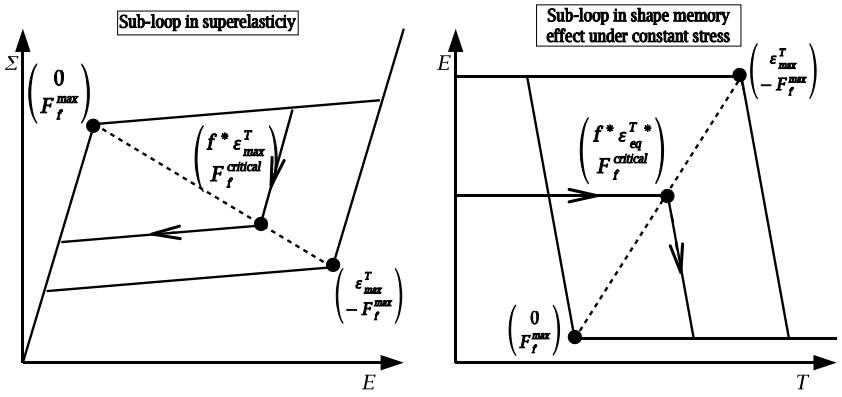

Fig. 5. Partial loading in superelasticity and shape memory effect under constant stress. Beginning of the forward transformation in dashed line, build from experimental considerations.

expression (33) of the critical transformation force is modified to be function of the fraction f^* and the mean transformation strain $\bar{\varepsilon}^{T*}_{eq}$ at the beginning of the forward loop (Fig. 5a and b):

$$F_f^{\text{critical}} = F_f^{\max}\left(1 - 2\frac{f^*\bar{\varepsilon}^{T*}_{eq}}{\varepsilon^{T}_{\max}}\right) \tag{34}$$

This expression of the critical transformation force does not introduce any supplementary parameters: the critical transformation force is defined from $F_f^{\max}$ which is the value describing the major loop.

4. Implementation in a FE code

The finite element method (FEM) is a very useful numerical tool to determine the response of a structure. But materials with multiphysics coupling and non-linear behaviour such as SMAs are not currently fully implemented in industrial software. We propose to implement the model previously presented into a finite element code in order to design SMA structures and actuators. The FE code ABAQUS proposes a tool called UMAT for User MATerial subroutine, useful to implement the behaviour of a material which is not in the standard database.

In the present work, the model was determined considering the stress and the temperature as control variables. So the behaviour law must be converted to use the natural control variables of the finite element method which are the total strain and the temperature. The increments of the stress and the internal variables are computed using a fully implicit scheme. The hypothesis of proportional loadings allow us to solve the equations of the implicit problem literally (see next paragraphs) and to express the consistent tangent stiffness matrix. The Umat subroutine developed in this work, is decomposed into two major steps (Fig. 6): detection of the activated mechanisms followed by a computation of the material response. During the first step, the thermodynamical forces are estimated by an elastic prediction. Then the appropriated behaviour is selected

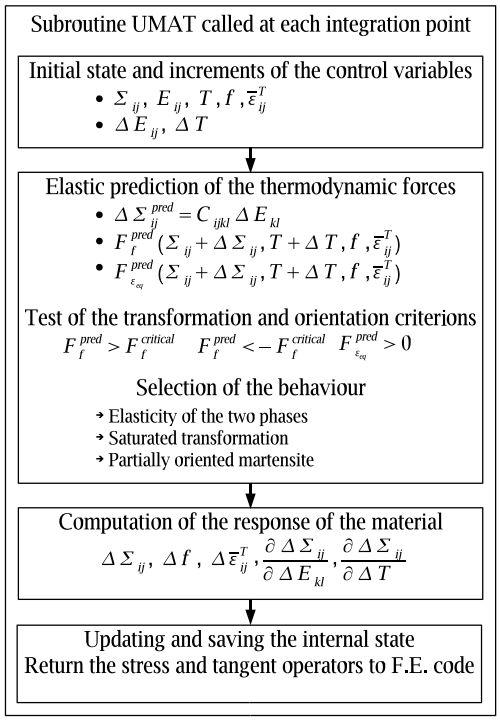

Fig. 6. Structure of the UMAT subroutine.

from one of the three classes (see Section 3.3). In a second step, the response of the material and the consistent tangent operators are computed corresponding to the selected behaviour.

4.1. Selection of the behaviour

Starting from an equilibrated state ($-F_f^{\text{critical}} \leqslant F_f \leqslant F_f^{\text{critical}}$ and $F_{\varepsilon_{\text{eq}}} \leqslant 0$), the control variables are incremented ($E_{ij} + \Delta E_{ij},\ T + \Delta T$). To determine in which class of behaviour the material will be at the end of the increment, the evolution of the thermodynamic forces are predicted for an elastic increment.

This elastic increment of stress is given by:

$$\Delta\Sigma_{ij}^{\text{pred}} = C_{ijkl}\Delta E_{kl} \tag{35}$$

where C_{ijkl} is the tensor of elasticity.

The thermodynamic forces associated to this new loading state are computed:

$$\begin{cases} F_f^{\text{pred}}\left(\Sigma_{ij} + \Delta\Sigma_{ij}^{\text{pred}}, T + \Delta T, f, \bar{\varepsilon}_{ij}^{\text{T}}\right) \\ F_{\varepsilon_{\text{eq}}}^{\text{pred}}\left(\Sigma_{ij} + \Delta\Sigma_{ij}^{\text{pred}}, T + \Delta T, f, \bar{\varepsilon}_{ij}^{\text{T}}\right) \end{cases} \tag{36}$$

These predicted forces allow to select the appropriated behaviour:

- IF ($F_{\varepsilon_{\text{eq}}}^{\text{pred}} > 0$ and ($-F_f^{\text{critical}} < F_f < F_f^{\text{critical}}$ or $f = 1$)) THEN orientation of the martensite without transformation (behaviour (3)).
- IF ($F_f^{\text{pred}} \geqslant F_f^{\text{critical}}$) THEN direct transformation
  - IF ($F_{\varepsilon_{\text{eq}}}^{\text{pred}} \geqslant 0$) THEN direct transformation and orientation of the martensite (behaviour (3)).
  - IF ($F_{\varepsilon_{\text{eq}}}^{\text{pred}} < 0$ or $\bar{\varepsilon}_{\text{eq}}^{\text{T}} = \varepsilon_{\text{max}}^{\text{T}}$) THEN direct transformation with fully oriented martensite (behaviour (2)).
- IF ($F_f^{\text{pred}} \leqslant -F_f^{\text{critical}}$) THEN forward transformation
  - IF ($F_{\varepsilon_{\text{eq}}}^{\text{pred}} \geqslant 0$) THEN forward transformation and orientation of the martensite (behaviour (3)).
  - IF ($F_{\varepsilon_{\text{eq}}}^{\text{pred}} < 0$ or $\bar{\varepsilon}_{\text{eq}}^{\text{T}} = \varepsilon_{\text{max}}^{\text{T}}$) THEN forward transformation with fully oriented martensite (behaviour (2)).
- ELSE elastic behaviour (1).

Once the behaviour of the material during the loading is defined, the evolution of the internal variables, the increment of the stress and the tangent modulus are computed.

4.2. Elasticity: behaviour (1)

When the transformation and the orientation criterion are not satisfied, the behaviour is elastic. The internal variables are kept constant:

$$\Delta f = 0 \tag{37}$$

$$\Delta\bar{\varepsilon}_{ij}^{\text{T}} = 0 \tag{38}$$

$$\Delta\Sigma_{ij} = C_{ijkl}\Delta E_{kl} \tag{39}$$

The tangent operators are the elastic one:

$$\frac{\partial\Delta\Sigma_{ij}}{\partial\Delta E_{kl}} = C_{ijkl} \quad \text{and} \quad \frac{\partial\Delta\Sigma_{ij}}{\partial\Delta T} = 0 \tag{40}$$

The elasticity is assumed identical for the two phases (see Section 2.1). For a linear, isotropic and homogeneous material, only the two Lame coefficients (μ, λ) are necessary:

$$C_{ijkl} = \mu(\delta_{ik}\delta_{jl} + \delta_{il}\delta_{jk}) + \lambda\delta_{ij}\delta_{kl} \tag{41}$$

4.3. Saturated transformation: behaviour (2)

In that case, the transformation criterion is satisfied while the mechanism of orientation of the martensite is not active or while transformation strain is saturated $\bar{\varepsilon}_{\text{eq}}^{\text{T}} = \varepsilon_{\text{max}}^{\text{T}}$. The equivalent mean transformation strain is kept constant while its direction still respects the rule of proportional loading (31):

$$\Delta\bar{\varepsilon}_{ij}^{\text{T}} = 0 \tag{42}$$

The thermodynamic balance must be verified at the beginning and at the end of the increment. The only activated mechanism is the transformation:

$$F_f\left(\Sigma_{ij}, T, f, \bar{\varepsilon}_{ij}^{\text{T}}\right) = \pm F_f^{\text{critical}} \tag{43}$$

$$F_f\left(\Sigma_{ij} + \Delta\Sigma_{ij}, T + \Delta T, f + \Delta f, \bar{\varepsilon}_{ij}^{\text{T}}\right) = \pm F_f^{\text{critical}} \tag{44}$$

The martensitic fraction is not saturated so the Lagrange multipliers λ_0 and λ_1 are null. The difference between relation (44) and (43) gives:

$$\Delta S_{ij}\bar{\varepsilon}_{ij}^{\text{T}} - B\Delta T - \left(H_{\text{grain}}\bar{\varepsilon}_{ij}^{\text{T}}\bar{\varepsilon}_{ij}^{\text{T}} + H_{\text{variant}}\right)\Delta f = 0 \tag{45}$$

The Hooke's law must also be satisfied:

$$\Delta\Sigma_{ij} = C_{ijkl}\left(\Delta E_{kl} - \bar{\varepsilon}_{kl}^{\text{T}}\Delta f\right) \tag{46}$$

From relations (45) and (46) the increment of martensitic fraction and the increment of stress are expressed as:

$$\Delta f = \frac{\bar{\varepsilon}^{\mathrm{T}}_{mn}\widetilde{C}_{mnpq}\Delta E_{pq} - B\Delta T}{H_{\mathrm{variant}} + \bar{\varepsilon}^{\mathrm{T}}_{mn}\widetilde{C}_{mnpq}\bar{\varepsilon}^{\mathrm{T}}_{pq} + H_{\mathrm{grain}}\bar{\varepsilon}^{\mathrm{T}}_{mn}\bar{\varepsilon}^{\mathrm{T}}_{mn}} \tag{47}$$

$$\Delta\Sigma_{ij} = \frac{\partial\Delta\Sigma_{ij}}{\partial\Delta E_{kl}}\Delta E_{kl} + \frac{\partial\Delta\Sigma_{ij}}{\partial\Delta T}\Delta T \tag{48}$$

The tangent operators are defined as:

$$\frac{\partial\Delta\Sigma_{ij}}{\partial\Delta E_l} = C_{ijpq}\left(I_{pqkl} - \frac{\bar{\varepsilon}^{\mathrm{T}}_{mn}\widetilde{C}_{mnkl}\bar{\varepsilon}^{\mathrm{T}}_{pq}}{H_{\mathrm{variant}} + \bar{\varepsilon}^{\mathrm{T}}_{mn}\widetilde{C}_{mnpq}\bar{\varepsilon}^{\mathrm{T}}_{pq} + H_{\mathrm{grain}}\bar{\varepsilon}^{\mathrm{T}}_{mn}\bar{\varepsilon}^{\mathrm{T}}_{mn}}\right) \tag{49}$$

$$\frac{\partial\Delta\Sigma_{ij}}{\partial\Delta T} = \frac{\widetilde{C}_{ijmn}\bar{\varepsilon}^{\mathrm{T}}_{mn}B}{H_{\mathrm{variant}} + \bar{\varepsilon}^{\mathrm{T}}_{mn}\widetilde{C}_{mnpq}\bar{\varepsilon}^{\mathrm{T}}_{pq} + H_{\mathrm{grain}}\bar{\varepsilon}^{\mathrm{T}}_{mn}\bar{\varepsilon}^{\mathrm{T}}_{mn}} \tag{50}$$

noting $\widetilde{C}_{ijkl} = C_{ijkl} - \delta_{ij}\frac{Cppkl}{3}$ the deviatoric elastic modulus, written for a linear, isotropic and homogeneous elasticity:

$$\widetilde{C}_{ijkl} = \mu\left(\delta_{ik}\delta_{jl} + \delta_{il}\delta_{jk} - \frac{2}{3}\delta_{ij}\delta_{kl}\right) \tag{51}$$

This behaviour is used in particular when computing superelastic loads.

4.4. Partially oriented martensite: behaviour (3)

In this case the two thermodynamic forces are activated. Moreover the internal variables are not saturated and every Lagrange multiplier as null. The thermodynamic balance must be verified at the beginning and at the end of the increment and by difference gives:

$$\begin{cases} (S_{ij}+\Delta S_{ij})\left(\bar{\varepsilon}^{\mathrm{T}}_{ij}+\Delta\bar{\varepsilon}^{\mathrm{T}}_{ij}\right) - S_{ij}\bar{\varepsilon}^{\mathrm{T}}_{ij} - B\Delta T - H_{\mathrm{variant}}\Delta f \\ \quad -H_{\mathrm{grain}}\left(\left(\bar{\varepsilon}^{\mathrm{T}}_{ij}+\Delta\bar{\varepsilon}^{\mathrm{T}}_{ij}\right)\left(\bar{\varepsilon}^{\mathrm{T}}_{ij}+\Delta\bar{\varepsilon}^{\mathrm{T}}_{ij}\right)(f+\Delta f) - \bar{\varepsilon}^{\mathrm{T}}_{ij}\bar{\varepsilon}^{\mathrm{T}}_{ij}f\right) = \pm F_f^{\mathrm{critical}} \\ \Delta S_{ij} - H_{\mathrm{grain}}\left(\left(\bar{\varepsilon}^{\mathrm{T}}_{ij}+\Delta\bar{\varepsilon}^{\mathrm{T}}_{ij}\right)(f+\Delta f) - \bar{\varepsilon}^{\mathrm{T}}_{ij}f\right) = 0 \end{cases} \tag{52}$$

Hooke's law must be satisfied:

$$\Delta\Sigma_{ij} = C_{ijkl}\left(\Delta E_{kl} - \left(\left(\bar{\varepsilon}^{\mathrm{T}}_{ij} + \Delta\bar{\varepsilon}^{\mathrm{T}}_{ij}\right)(f+\Delta f) - \bar{\varepsilon}^{\mathrm{T}}_{ij}f\right)\right) \tag{53}$$

Resolution of the system (52) with the elastic relation (53) gives the increments of volume fraction, the mean transformation strain increment and the stress increment:

$$\Delta f = \frac{-B\Delta T}{H_{\mathrm{variant}}} \tag{54}$$

$$\Delta\bar{\varepsilon}^{\mathrm{T}}_{ij} = \left(\widetilde{C}_{ijmn} + H_{\mathrm{grain}}I_{ijmn}\right)^{-1}\widetilde{C}_{mnkl}\Delta E_{kl} - \bar{\varepsilon}^{\mathrm{T}}_{ij}\frac{\Delta f}{f+\Delta f} \tag{55}$$

$$\Delta\Sigma_{ij} = \frac{\partial\Delta\Sigma_{ij}}{\partial\Delta E_{kl}}\Delta E_{kl} \tag{56}$$

The tangent operators turn to be:

$$\frac{\partial\Delta\Sigma_{ij}}{\partial\Delta E_{kl}} = C_{ijpq}\left(I_{pqkl} - \left(\widetilde{C}_{pqmn} + H_{\mathrm{grain}}I_{pqmn}\right)^{-1}\widetilde{C}_{mnkl}\right) \tag{57}$$

$$\frac{\partial\Delta\Sigma_{ij}}{\partial\Delta T} = 0 \tag{58}$$

The relations (55) and (56) are easily extended to the case of saturation of the transformation $f = 1$, where they are directly used with $\Delta f = 0$.

This behaviour is involved when computing reorientation of martensite and shape memory cycles.

5. Computed behaviour

To validate the implementation of the model into the FE code, different loadings have been computed for a single cubic element. Numerical results for superelasticity and shape memory effect under constant stress are successfully compared with experimental results from the literature. Application on a bending test, shows the capacities of the model for structure analysis.

5.1. Characterization tests

The model is tested on a simple 3D cubic element. A uniform mechanical and thermal loading is imposed over the entire element. The material coefficients are those of a Cu Al—11.6 Be—0.5 polycrystal (Table 1). Results are compared with tensile tests performed by Entemeyer (1996) on a superelastic wire.

Table 1
Material coefficients for the Cu Al—11.6 Be—0.5 (Entemeyer, 1996)

E	v	T_0	B	$\bar{\varepsilon}^{\mathrm{T}}_{\max}$	F_f^{critical}	H_{variant}	H_{grain}
70 000 MPa	0.3	−12.5 °C	0.066 MPa/°C	0.03	1.2 MPa	0.5 MPa	2100 MPa

The material parameters T_0, F_f^{critical} and H_{variant} have been determined from the transformation temperatures M_s, M_f and A_f:

$$T_0 = \frac{M_s + A_f}{2}$$
$$F_f^{\text{critical}} = B(M_s - T_0)$$
$$H_{\text{variant}} = B(M_f - M_s)$$

Parameters like elastic constants (E, ν), maximal transformation strain $\varepsilon_{\max}^{\text{T}}$ and stress–temperature sensitivity B has been taken from the literature. Intergranular and intervariant parameters H_{grain} and H_{variant} were the only adjusted ones.

Superelastic loadings (Fig. 7) are performed for three temperatures and shape memory effect under constant stress (Fig. 8) are drawn for three different stress levels. Results show that the model is close to experimental results. In shape memory effect under constant stress, evolution of the transformation strain with the level of applied stress is well captured. The description of partial loadings in the proposed model, appears very suitable to catch the evolution of the wide of the hysteresis with the level of applied stress.

A more complex loading path is also tested: a shape memory cycle followed by a constraint recovery. It appends in three steps (Fig. 9):

1. Conditioning of the element in martensitic phase: a displacement Δ_0 is imposed.
2. Self-deformation of the element by heating, producing a free recovery of the clearance $\Delta_{\text{clearance}}$ between the element in SMA and its neighbourhood.
3. Stress generation if the shape recovery is constrained by the obstacle ($\Delta_{\text{clearance}} < \Delta_0$).

A computed typical response is shown in the space (Σ, E, T) (Fig. 10). One can observe a linear

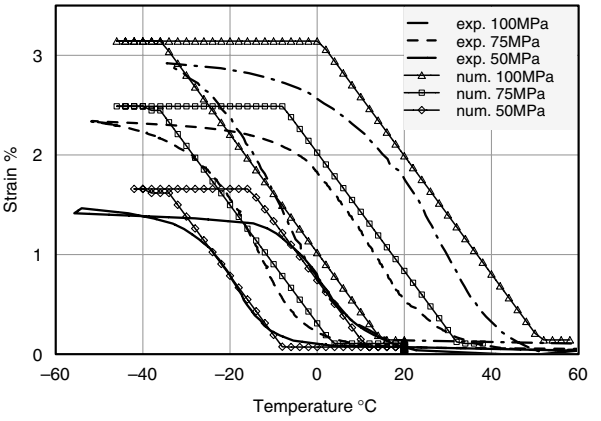

Fig. 8. Shape memory effect under constant stress. Experiments and simulations at different stress levels.

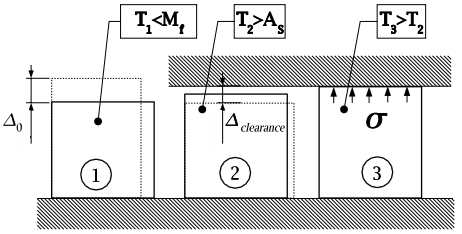

Fig. 9. Shape memory cycle. 1—Conditioning in martensitic phase with an imposed displacement Δ_0. 2—Free recovery of the clearance $\Delta_{\text{clearance}}$. 3—Constrain recovery ($\Delta_{\text{clearance}} < \Delta_0$).

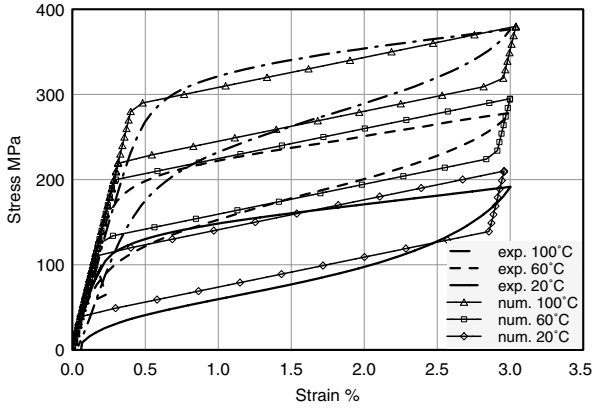

Fig. 7. Superelastic tensile tests and computations at different temperatures.

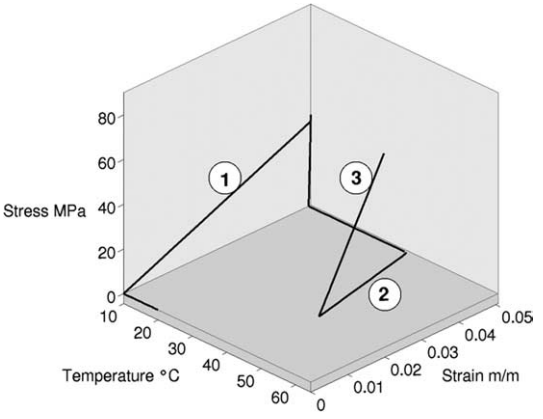

Fig. 10. Computed shape memory cycle defined in Fig. 9.

Table 2
Material coefficients for the Cu Al—11.4 Be—0.6 (Gillet et al., 1995)

E	ν	T_0	B	$\bar{\varepsilon}^T_{\max}$	F_f^{critical}	H_{variant}	H_{grain}
70 000 MPa	0.3	−97.5 °C	0.066 MPa/°C	0.03	0.735 MPa	2 MPa	7700 MPa

behaviour during reorientation, a free shape recovery during the clearance compensation and finally a stress generation when the element reaches contact with the obstacle.

These different results show a satisfactory implementation of the shape memory constitutive law into the finite element code.

5.2. Structure computation

In this section, the numerical computation of a three point bending of a superelastic beam is compared with experimental results and an analytical model developed by Gillet et al. (1995).

The material parameters employed in the computation (Table 2) are the same as the ones used by Gillet for his analytical model. They were determined on a uniaxial tensile test performed at the same temperature as the bending test.

Plane strain elements are used to mesh the beam in its length and in its thickness. Due to the symmetry of the problem, the computation is performed on half the beam (Fig. 11).

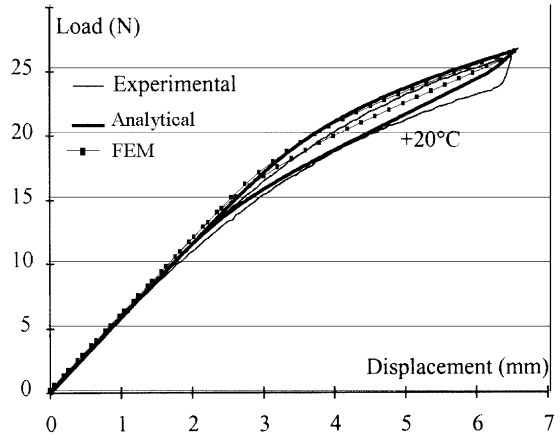

Fig. 12. Experimental, analytical and FEM response of the superelastic beam.

The load–displacement curve computed shows a good estimation of the observed behaviour (Fig. 12).

Differences with the experimental result are observed on the unloading for both the numerical and the analytical models. It takes the origin in a

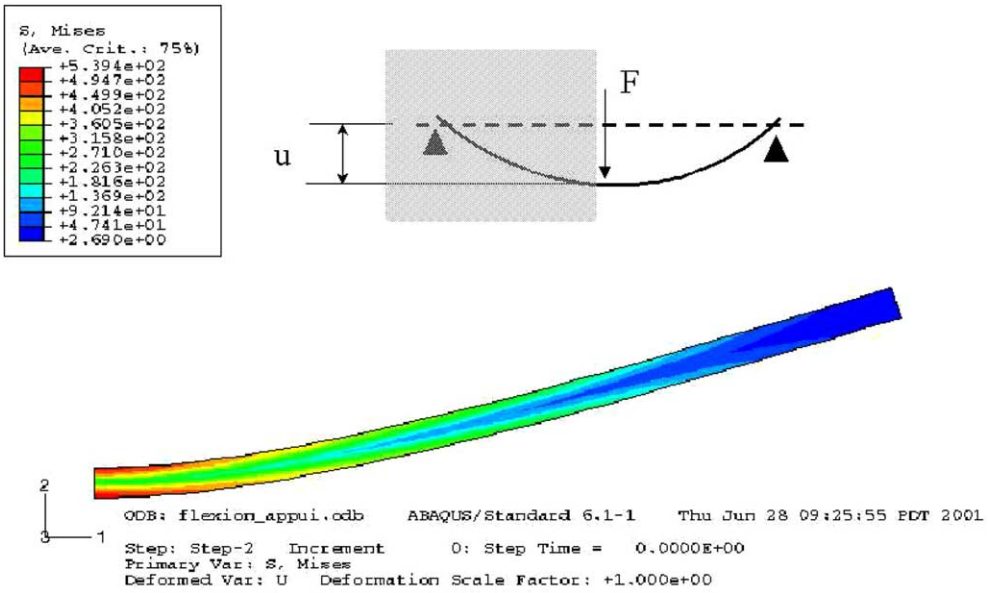

Fig. 11. Geometry of the beam. Isovalues of the Mises equivalent stress [0–540 MPa].

sliding occurring between the beam and the contact points, that has not been introduced in the modelling. Differences between analytical and FEM results come mainly from the different choices in the description of the transforming regime. Gillet's analytical model uses a parabolic approximation while a linear one is used in the present work. Differences also originate from the transformation criterion used: a symmetric J_2 type in this paper and a J_2/J_3 in Gillet's work. Stress cartography over the beam shows the symmetric repartition of the stress between tension and compression (Fig. 11) that is far from the experiment (Bouvet et al., 2002).

6. Conclusion

Description of the different behaviours in shape memory alloy are unified into a single formulation including superelasticity, shape memory effect and reorientation of the martensitic phase. The model is based on the physics of the martensitic transformation. Its analytical formalism is well adapted to numerical simulation of structures using the finite element method. Computation on single element with uniform loading validate the implementation. But the application on a structure shows the limits and suggests improvements. More complex loadings and structures have to be tested.

The model is adapted to systems working with complete martensitic transformation. The global response of the system is validated but locally at the beginning and at the end of the transformation the prediction is not precise. Furthermore, the singular points of the behaviour law when appending a large modification of the rigidity provide numerical difficulties and cause convergence problems. A solution would be the use of non-linear transformation law. The tension–compression asymmetry is a fundamental characteristic of the SMA (Liu et al., 1998; Orgeas and Favier, 1998). In many structures, where the two kinds of loads coexist, it is necessary to introduce this asymmetry to compute precise results. Finally improvements of the prediction power of the model will come from a more precise analysis of the internal energy of the RVE.

Other behaviours of the SMA are not modelled in this study such as the two way memory effect, the influence of cycling on the transformation limits or the damping effect. Nevertheless most of the applications in SMA can be simulated. And that kind of model would help in engineering smart systems.

References

Atanackovic, T., Achenbach, M., 1989. Moment–curvature relations for a pseudoelastic beam. Continuum Mech. Thermodyn., 73.

Auricchio, F., Taylor, R.L., 1997. Shape-memory alloys: modelling and numerical simulations of the finite-strain superelastic behavior. Comput. Methods Appl. Mech. Eng. 143, 175–194.

Bekker, A., Brinson, L.C., 1998. Phase diagram based description of the hysteresis behaviour of shape memory alloy. Acta Metall. 46 (10), 3649–3665.

Bouvet, C., Calloch, S., Lexcellent, C., 2002. Mechanical behavior of a Cu–Al–Be shape memory alloy under multiaxial proportional and non proportional loadings. J. Eng. Mat. Tech. 124, 112–123.

Entemeyer, D., 1996. Etude micromécanique du comportement thermomécanique des AMF. PhD thesis, Université de Metz, France.

Gillet, Y., Patoor, E., Berveiller, M., 1995. Calculation of pseudoelastic elements using a non symmetrical thermomechanical transformation criterion and associated rule. J. Int. Mat. Syst. Struct. 9 (5), 366–378.

Hwang, S.C., Lynch, S.C., McMeeking, R.M., 1995. Ferroelectric/ferroelastic interactions and a polarization switching model. Acta Metall. Mater. (43), 2073–2084.

Kröner, E., 1961. Plastischer Verformung des Vielkristalls. Acta Metall. 9, 155–161.

Lagoudas, D.C., Bo, Z., 1999. Thermomechanical modeling of polycrystalline SMAs under cyclic loading, Part I, II, III and IV. Int. J. Ing. Sci. (37), 1089–1249.

Leclercq, S., Lexcellent, C., 1996. A general macroscopic description of the thermomechanical behaviour of shape memory alloys. J. Mech. Phys. Solids 44 (6), 953–980.

Lim, T.J., McDowell, D.L., 2002. Cyclic thermomechanical behavior of a polycrystalline pseudoelastic shape memory alloy. J. Mech. Phys. Sol. (50), 651–676.

Liu, Y., Xie, Z., Humbeeck, J., Delaey, L., 1998. Asymmetry of stress–strain curves under tension and compression for NiTi shape memory alloys. Acta Metall. 46 (12), 4325–4338.

Maugin, G.A., 1988. Continuum Mechanics of Electromagnetic Solids. Elsevier Science Publishers, Amsterdam.

Niclaeys, C., Ben Zineb, T., Arbab Chirani, S., Patoor, E., 2002. Determination of the interaction energy in the martensitic state. Int. J. Plast. (18), 1619–1647.

Orgeas, L., Favier, D., 1998. Stress-induced martensitic transformation of a NiTi alloy in isothermal shear, tension and compression. Acta Mater. 46 (15), 5579–5591.

Patoor, E., Eberhardt, A., Berveiller, M., 1988. Thermomechanical behaviour of shape memory alloy. Arch. Mech. 40 (5–6), 775–794.

Patoor, E., Eberhardt, A., Berveiller, M., 1996. Micromechanical modelling of superelasticity in shape memory alloys. J. Phys. IV, col. C1 6, 277–292.

Siredey, N., Patoor, E., Berveiller, M., Eberhardt, A., 1999. Constitutive equations for polycrystalline thermoelastic shape memory alloys. Part I. Intragranular interactions and behaviour of the grain. Int. J. Solids Struct. 36, 4289–4315.

Tanaka, K., Nishimura, F., Hayashi, T., Tobushi, H., Lexcellent, C., 1995. Phenomenological analysis on subloops and cyclic behaviour in shape memory alloys under mechanical and/or thermal loads. Mech. Mater. 19, 281–292.

Thamburaja, P., Anand, L., 2002. Superelastic behavior in tension–torsion of an initially textured Ti–Ni shape memory alloy. Int. J. Plasticity (18), 1607–1617.

Tobushi, H., Tanaka, K., 1991. Deformation of a shape memory alloy helical spring. JSME Int. J., Ser. 1 34 (1), 83.

Trochu, F., Qian, Y.-Y., 1997. Nonlinear finite element simulation of superelastic shape memory alloy parts. Comput. Struct. 62 (5), 799–810.

Wu, X.D., Sun, G.J., Wu, J.S., 2003. The nonlinear relationship between transformation strain and applied stress for nitinol. Mater. Lett. (57), 1334–1338.

Zhang, S., McCormick, P.G., 2000. Thermodynamic analysis of shape memory phenomena—II. Modelling. Acta Mater. 48, 3091–3101.